Published in final edited form as:
*J Neuropathol Exp Neurol*. 2008 October ; 67(10): 976–983. doi:10.1097/NEN.0b013e318187a279.

# Interleukin 10 Protects the Brain Microcirculation From Spirochetal Injury

**Diana Londoño, MD**, **Jenny Carvajal**, **Carolina Arguelles-Grande, MD**, **Adriana Marques, MD**, and **Diego Cadavid, MD**
From the Department of Neurology and Neuroscience and Center for Emerging Pathogens at UMDNJ-New Jersey Medical School (DL, JC, CA-G, DC), Newark, New Jersey; and Clinical Studies Unit (AM), Laboratory of Clinical Infectious Diseases, National Institute of Allergy and Infectious Diseases, National Institutes of Health, Bethesda, Maryland.

## Abstract

Spirochetal infections are an important cause of neurological disease. In previous studies of the pathogenesis of spirochetal brain infection, mice inoculated with *Borrelia turicatae*, an agent of tick-borne relapsing fever in North America, developed mild meningitis and parenchymal activation/infiltration by interleukin 10 (IL-10)-producing microglia/macrophages. Here, we investigated the neuro-protective effects of IL-10 during spirochetal infection by comparing the outcomes of *B. turicatae* infection in wild-type and IL-10-deficient RAG2-deficient mice. Mice were infected with either serotype 1 (Bt1), which causes more brain infection but lower bacteremia, or Bt2, which causes less brain infection but higher bacteremia. Interleukin 10 deficiency resulted in early death from subarachnoid/intraparenchymal brain hemorrhage in Bt2-infected mice. These mice had marked apoptosis of brain microvascular endothelial cells as assessed by terminal transferase-mediated DNA nick end-labeling staining. In contrast, Bt1 infection caused milder subarachnoid hemorrhage. Neuronal apoptosis was observed in mice infected with both serotypes and was prominent in the cerebellum. Neutralization of tumor necrosis factor prevented death and reduced morbidity and brain injury in mice infected by both serotypes. We conclude that IL-10 plays a critical role protecting the cerebral microcirculation from spirochetal injury possibly by inhibition effects of tumor necrosis factor.

### Keywords

Apoptosis; *Borrelia*; Endothelial cell; Interleukin 10; Neuroprotection; Spirochete infection; Tumor necrosis factor

## INTRODUCTION

Neurological disease is an important complication of infection with pathogenic spirochetes, including the agents of syphilis (1), relapsing fever (2–4), and Lyme disease (5). Little is known about the pathogenesis of neurological complications of spirochetal infections in part because animal models of syphilis (6) and Lyme disease (7–12) lack brain involvement features. In contrast, brain involvement is a frequent feature in animal models of relapsing fever (4). Our laboratory studies the pathogenesis of spirochetal brain infection in mice infected with *Borrelia*



Send correspondence and reprint requests to: Diego Cadavid, MD, UMDNJ-New Jersey Medical School, Newark, NJ 07103; E-mail: E-mail: cadavidi@umdnj.edu.
Dr Cadavid is now with the Experimental Neurology Group, Biogen Idec, Cambridge, MA.

*turicatae*, an agent of relapsing fever in North America (13–17). Previous studies have shown that spirochetes readily infect the brain early after systemic inoculation and preferentially localize to the leptomeninges (15,16,18). Although the host immune response usually clears spirochetes from blood and brain via serotype-specific antibodies, spirochetes occasionally escape killing in the brain resulting in residual brain infection (19,20). In the absence of B cells, persistent infection is the rule (13,14,16,17,21). Pathological examination of infected brains reveals mild meningitis and microglial activation (13,17,21), but neither residual brain infection or persistent infection in B cell-deficient mice results in brain injury (1,17,19,21).

Humans with epidemic relapsing fever borreliosis have very high levels of circulating interleukin 10 (IL-10) at times of preserved neurological function (22), suggesting that IL-10 may be neuroprotective in spirochetal infection. This notion is supported by our recent finding that mice persistently infected with *B. turicatae* also produce large amounts of IL-10 in blood and brain and have no apparent brain injury (13,21). In this study, we investigated whether IL-10 protects the brain from spirochetal injury by comparing the outcome of infection with *B. turicatae* in IL-10-deficient (RAG2/IL-$10^{-/-}$) and control ($RAG2^{-/-}$) mice. $RAG2^{-/-}$ mice were used to avoid serotype clearance and to compare the effects of serotypes of different systemic virulence and neurotropism over time (13,15,16,21,23,24).

## MATERIALS AND METHODS

### Strains and Culture Conditions

Isogenic serotypes 1 (Bt1) and 2 (Bt2) of *B. turicatae* have been previously characterized (18,25,26). Spirochetes were cultured in BSK-H media (Sigma Chemical Co, St Louis, MO) with 6% rabbit serum. Before infection, *Borrelia* viability was assessed by phase-contrast microscopy, and serotype identity was confirmed by Western blot with Vsp-specific monoclonal antibodies 5F12 for Bt2 and IH12 for Bt1 (25,26).

### Mouse Infections

Female 4- to 5-week-old C57BL/10SgSnAi-[KO] RAG2 ($RAG2^{-/-}$) and IL-10/RAG2 double-deficient (IL-10/$RAG2^{-/-}$) mice were generated by crossing C57BL/10SgSnAi-[KO]IL-10 and C57BL/10SgSnAi-[KO]RAG2 mice obtained from Taconic Farms (Germantown, NY) (27). The mice were inoculated intraperitoneally with $10^3$ Bt1 or Bt2 spirochetes in 200 μL of PBS or with PBS alone as a control. Groups of 3 to 8 mice each were used for all experiments. Mice were maintained under specific pathogen-free conditions. Housing and care was in accordance with the Animal Welfare Act in facilities accredited by the Association for Assessment and Accreditation of Laboratory Animal Care. Killing and necropsy followed by intracardiac perfusion with buffer to minimize blood contamination were performed as in previous studies (16,18). To measure infection in the blood, spirochetes were counted in necropsy plasma by phase-contrast microscopy on a Petroff-Hausser chamber.

### Clinical Examination

The onset and severity of clinical disease was assessed by an investigator masked to mouse genotype and infection (Diana Londoño) using the following clinical scoring system: 1) vestibular dysfunction (spinning while held up by the tail): none, 0; unsustained, 1; sustained, 2; 2) skin disease (fur ruffling): normal, 0; ruffled, 1; ruffled and dry, 2; 3) ocular disease (conjunctival secretion): none, 0; mucous, 1; purulent, 2; 4) inactivity (lack of spontaneous walking): none, 0; mild, 1; moderate to severe, 2.

## Pathology

For histological analyses, tissues were fixed in 4% paraformaldehyde overnight at 4°C, paraffin-embedded, and stained with hematoxylin and eosin (H and E). Apoptosis was studied using the terminal transferase-mediated DNA nick end-labeling (TUNEL) assay as previously described (23). Cells with distinct nuclear staining were considered TUNEL positive. To compare the severity of apoptosis among mouse groups, an examiner (Diana Londoño) counted TUNEL-positive cells per $mm^2$ in 5 consecutive 100× microscopic fields in the cerebellum (molecular layer) and leptomeninges (over the brain convexity). For immunofluorescence, TUNEL-positive cells were labeled with biotinylated-conjugated dUTP using TdT as described before and visualized with tetramethyl rhodamine iso-thiocyanate-streptavidin diluted 1/1000 (Invitrogen, Carlsbad, CA). For endothelial cell staining, sections were blocked with 5% casein solution plus 10% rabbit serum and incubated overnight with 1 μg/mL of fluorescein isothiocyanate-labeled isolectin B4 (Sigma Chemical Co). Images were obtained with an Olympus BX40 microscope with an Optronics 1.3 megapixel digital camera using single fluorescein isothiocyanate or tetramethyl rhodamine isothiocyanate filters and merged with Adobe Photoshop.

## TaqMan Reverse Transcription-Polymerase Chain Reaction

Total RNA was extracted from 100 mg of half-brain homogenates (FastPrep24 homogenizer, MP Biomedicals, Irvine, CA) using the phenol/chloroform method followed by DNAse treatment (Ambion Kit, Applied Biosystems, Foster City, CA). RNA was quantified with a Nanodrop using the A260/A280 ratio. One microgram of RNA per sample was reverse transcribed with random hexamers using the Transcriptor First Strand complementary DNA Synthesis Kit (Roche Applied Science, Penberg, Germany) in 20-μL reaction volumes. Quantitative real-time polymerase chain reaction was performed on an ABI Prism 7500 Sequence Detection System (Applied Biosystems) in multiplex using 10% of each complementary DNA in 50 μL-reaction volumes with TaqMan Universal master mix (Applied Biosystems) and standard conditions for 40 cycles. The primers and probes for the relative quantification of the pathogen load were borrelial 16S ribosomal RNA (rRNA) (13) and mouse 18S rRNA (4319413E, Applied Biosystems) as endogenous control for input brain RNA. The standard curve used log 10 dilutions of DNA prepared from a known number of cultured spirochetes in 100 ng of uninfected mouse brain complementary DNA in triplicate. Analysis was done by extrapolation of the sample data to the standard curve. The rRNA 16S expression value was normalized to the mouse rRNA 18S expression.

## Cytokines

The concentration of tumor necrosis factor (TNF) in necropsy plasma was measured with the Luminex 100 Multi-Analyte Profiling System (Luminex Corp, Austin, TX) using BioPlex Manager software (Bio-Rad Laboratories, Hercules, CA) with Lincoplex cytokine assay kits (Linco Research, St Charles, MO). For neutralization of TNF, mice were injected intraperitoneally with 0.75 mg of neutralizing monoclonal antibody MP6-XT22/11 against mouse TNF (kind gift from Drs Carl Feng and Alan Sher, National Institute of Allergy and Infectious Diseases, Bethesda, MD) (28,29). The antibody was administered 2 hours before infection and 5 days later.

## Statistical Analysis

All statistical analyses were performed using GraphPad PRISM 4 (GraphPad Software, La Jolla, CA). Data are presented as mean ± SD or median (range). The Mann-Whitney or unpaired *t*-test was used to compare data depending on the distribution. Results were considered statistically significant if $p < 0.05$ and highly statistically significant if $p < 0.01$.

# RESULTS

## Morbidity and Mortality

We first determined whether IL-10 deficiency influenced the development of clinical disease. Groups of six to eight 4-week-old female RAG2/IL-$10^{-/-}$ or RAG$2^{-/-}$ mice were inoculated intraperitoneally with $10^3$ Bt1 or Bt2 spirochetes or PBS as a control. We chose these isogenic serotypes because they differ in their pathogen load in blood and brain; that is, Bt1 causes more brain infection but lower bacteremia than Bt2 (13,15,17,21,23). The examiner scored all mice for clinical signs daily for up to 12 days as described in the Materials and Methods section. The findings were recorded on a scale of 0 to 2 (see Materials and Methods section) and expressed as sum disease severity scores per group per day. By Day 5 after inoculation, all infected RAG2/IL-$10^{-/-}$ mice developed clinical disease consisting of conjunctival discharge, vestibular dysfunction, fur ruffling, and inactivity that was more severe in Bt2-infected than Bt1-infected mice (Fig. 1). Only Bt2-infected RAG2/IL-$10^{-/-}$ mice began to die by Day 4 to 5 after inoculation and had to be killed. These mice had very high bacteremia and circulating levels of TNF, as reported in a separate publication (24). The Bt1-infected RAG2/IL-$10^{-/-}$ mice showed clinical signs but no mortality and were necropsied on Day 12 because of increased morbidity. Similar to Bt2 mice necropsied on Day 5 (24), the pathogen load in the blood of Bt1-infected mice necropsied on Day 12 was higher in RAG2/IL-$10^{-/-}$ than in RAG$2^{-/-}$ mice (Fig. 2). The circulating levels of TNF were also higher in these mice: the median (range) levels in picograms per milliliter were 62 (range, 26–92 pg/mL) in RAG2/IL-$10^{-/-}$ compared with 17 (range, 13–30 pg/mL) in RAG$2^{-/-}$ mice ($p < 0.01$). Unlike infected RAG2/IL-$10^{-/-}$ mice, none of the infected RAG$2^{-/-}$ mice or uninfected RAG2/IL-$10^{-/-}$ mice showed any signs of clinical disease or mortality over the 12-day observation period (data not shown). These results indicate that IL-10 protected mice from early clinical disease and mortality in this spirochetal infection.

## Brain Hemorrhage

At necropsy, 5 of 8 Bt2-infected RAG2/IL-$10^{-/-}$ mice had prominent subarachnoid and intraparenchymal brain hemorrhage (Table). None of the other organs showed any gross evidence of hemorrhage at necropsy. Microscopic examination of H and E-stained sections confirmed the presence of massive brain hemorrhage in 5 of 8 Bt2-infected RAG2/IL-$10^{-/-}$ mice: brain hemorrhages were variable in size, multiple, and commonly located in the cerebellum, but they involved all brain regions (Fig. 3A). There was prominent microvascular leptomeningeal vasculitis in 6 of 8 mice (Table): inflammatory cells, including monocytes and neutrophils, infiltrated leptomeningeal microvessels that were often surrounded by hemorrhages (Fig. 3B). None of the Bt2-infected RAG$2^{-/-}$ mice or uninfected RAG$2^{-/-}$ or RAG2/IL-$10^{-/-}$ mice showed evidence of brain hemorrhage or vasculitis at necropsy either grossly or microscopically (Table; Figs. 3C, D). Microscopic examination revealed small areas of hemorrhage in the mediastinum of 2 of 8 Bt2-infected RAG2/IL-$10^{-/-}$ mice, but there were no hemorrhages in the lungs, liver, kidney, spleen, or intestines in these mice. To confirm these results, we infected new groups of 3 RAG$2^{-/-}$ and 3 RAG2/IL-$10^{-/-}$ mice with Bt2 and necropsied them on Day 5 after inoculation. As before, we used extensive intracardiac perfusion with buffer to minimize blood contamination of tissues. Macroscopic examination revealed prominent brain hemorrhage in 2 of 3 RAG2/IL-$10^{-/-}$ mice and in 0 of 3 RAG$2^{-/-}$ mice, and none of the other organs showed evidence of hemorrhage on macroscopic examination. Using TaqMan reverse transcription-polymerase chain reaction, we determined that in association with hemorrhage, the mean number of spirochetes per nanogram brain RNA increased from 323 (SD ±345) in the 4 mice without hemorrhage to 7,291 (SD ±3,511) in the 2 mice with hemorrhage ($p < 0.05$), a 22-fold increase.

Brain hemorrhage in Bt1-infected RAG2/IL-10$^{-/-}$ mice was less frequent and milder than with Bt2 infection even though Bt1-infected mice were necropsied 1 week later, on Day 12 after inoculation (Table; Figs. 3E, F). Microscopic examination of the brain of Bt1-infected RAG2/IL-10$^{-/-}$ mice showed not only milder hemorrhage but also thrombosis of leptomeningeal microvessels (Table). Half of these mice also showed mild hemorrhages in kidneys, spleen, and/or intestines (data not shown). In contrast, none of the Bt1-infected RAG2$^{-/-}$ mice showed evidence of hemorrhage or thrombosis in the brain or any other organ. These data suggest that IL-10 protects the cerebral microcirculation from hemorrhage and thrombosis during spirochetal infection and that the brain microvasculature shows selective vulnerability to spirochetal injury.

## Brain TUNEL Staining

Because brain hemorrhage was more severe and bacteremia was higher in mice infected with Bt2, circulating spirochetes might be directly or indirectly responsible for damage to the cerebral microcirculation. We therefore studied the brains of RAG2/IL-10$^{-/-}$ mice for evidence of apoptosis in brain microvascular endothelial cells using TUNEL staining (23) and found prominent TUNEL staining of leptomeningeal endothelial cells in Bt2-infected RAG2/IL-10$^{-/-}$ mice (Figs. 4A, B, E–G); staining was much more apparent in areas of subarachnoid hemorrhage (Figs. 4A, B). Terminal transferase-mediated DNA nick end-labeling staining of leptomeningeal endothelial cells was much lower in Bt1-infected than in Bt2-infected mice and was very rarely seen in infected RAG2$^{-/-}$ mice (Figs. 4C, D). Brain apoptosis was apparently not restricted to leptomeningeal endothelial cells because frequent TUNEL-stained neurons were observed in the cerebellum (Fig. 4H), thalamus, and cerebral cortex (data not shown) of RAG2/IL-10$^{-/-}$ mice infected with either serotype. Terminal transferase-mediated DNA nick end-labeling-stained neurons were also observed in RAG2$^{-/-}$ mice infected with either serotype (Fig. 4I), whereas uninfected control mouse brains had only rare TUNEL-positive cells (data not shown). Quantification of TUNEL-stained endothelial cells in the leptomeninges and neurons in the molecular layer of the cerebellum confirmed that neuronal apoptosis of similar degree occurred in mice infected with either serotype, whereas leptomeningeal cell apoptosis was more extensive in Bt2-infected mice (Fig. 5). Thus, IL-10 seems to protect brain endothelial cells from apoptosis during severe spirochetal infection as assessed by TUNEL staining.

## Neutralization of TNF

Next we studied whether the neuroprotective role of IL-10 during spirochetal infection was caused by inhibitory effects on TNF. For this, we compared the outcome of infection in RAG2/IL-10$^{-/-}$ mice with or without neutralization of TNF. Groups of 6 RAG2/IL-10$^{-/-}$ mice were treated before inoculation with Bt1 or Bt2 and 5 days later with anti-TNF-neutralizing antibody, and a masked examiner (Diana Londoño) compared morbidity and mortality over 12 days. Unlike the previous experiment, none of the Bt2-infected RAG2/IL-10$^{-/-}$ mice died spontaneously in this experiment, and mice showed similar clinical disease severity scores with either serotype (Fig. 6). Macroscopic examination at necropsy revealed only small petechial brain hemorrhages in 1 of 6 mice infected with Bt1 and 2 of 6 mice infected with Bt2 (Table). Mild extraparenchymal hemorrhages were found in half of the mice infected with either serotype (data not shown). Microscopic examination of brain sections revealed small areas of subarachnoid hemorrhage without any detectable parenchymal hemorrhage (Fig. 3H). Vasculitis, thrombosis, and meningitis were, however, observed in mice infected with either serotype (Table; Figs. 3G, H). Examination of TUNEL-stained sagittal brain sections revealed that neutralization of TNF significantly decreased leptomeningeal cell staining in Bt2-infected mice ($p < 0.01$, Fig. 5B) and neuronal staining in Bt1-infected and Bt2-infected mice ($p < 0.05$, Figs. 5A, B). These data suggest that the protective role of IL-10 in spirochetal infection is mediated to a large extent by inhibition of TNF.

## DISCUSSION

The present results indicate that IL-10 plays a critical role protecting the cerebral microcirculation from injury during severe spirochetal infection. The major findings are as follows: 1) IL-10 deficiency in RAG2$^{-/-}$ mice infected with *B. turicatae* resulted in increased clinical disease, with higher bacteremia and systemic production of TNF; 2) IL-10 deficiency in Bt2-infected RAG2$^{-/-}$ mice resulted in early mortality from severe subarachnoid and intraparenchymal hemorrhage with prominent apoptosis of brain microvascular endothelial cells; 3) thrombosis of leptomeningeal micro-vessels was observed in mice after 12 days of infection with either serotype; 4) brain apoptosis as assessed by TUNEL staining was not limited to leptomeningeal microvascular endothelial cells but also involved neurons; 5) neutralization of TNF prevented mortality and reduced morbidity and brain injury in RAG2/IL-10$^{-/-}$mice infected with either serotype.

An intriguing finding was that in RAG2/IL-10$^{-/-}$ mice, infection resulted in severe hemorrhage in the brain but not in other organs, and that it occurred with Bt2 but not with Bt1 infection. Because the entire intravascular compartment is exposed to high numbers of circulating spirochetes, one would expect that all endothelial cells would be similarly affected, but both macroscopic examination at necropsy and microscopic examination of H and E-stained sections confirmed the preferential involvement of the cerebral microcirculation. This suggests that brain microvascular endothelial cells are more susceptible to spirochetal injury than endothelial cells elsewhere in the body. Because severe brain hemorrhage occurred with Bt2, which causes higher bacteremia (~$10^8$/mL) (24) than Bt1 (~$10^7$/mL, Fig. 2), this selective vulnerability may become apparent only with very high levels of bacteremia. Similarly, a positive correlation between brain hemorrhage and intensity of bacteremia has been reported in human relapsing fever (2). One possible explanation for this selective vulnerability is lower production of IL-10 in response to bacteremia by brain microvascular endothelial cells when compared with endothelial cells elsewhere in the body. Our recent observations that human brain microvascular endothelial cells did not produce any IL-10 when exposed to Bt2 in vitro and that Bt2 killing of brain microvascular endothelial cells significantly decreased in the presence of IL-10 are consistent with this view (unpublished data). Furthermore, in a previous study, we did not observe IL-10 staining in endothelial cells by immunohistochemistry in the brains of RAG1$^{-/-}$ mice persistently infected with Bt1 (13). Therefore, brain endothelial cells may be more dependent than other endothelial cells on systemic delivery of IL-10 for protection from spirochetal injury (e.g. through the blood). Confirmation of this hypothesis awaits direct comparative studies of IL-10 production and susceptibility to spirochetal injury of brain and nonbrain endothelial cells.

Similarly interesting was the finding that brain micro-vascular pathology was not only hemorrhagic but also thrombotic (Fig. 3F). In fact, blood vessel thrombosis was more common than hemorrhage in the brain of mice necropsied on Day 12 (Table). This observed thrombosis of cerebral microvessels may have contributed to the observed neuronal TUNEL staining (Fig. 4,Fig. 5). Because brain micro-vascular endothelial cell apoptosis was greater in Bt2 than in Bt1 infection and Bt2 caused higher bacteremia than Bt1, it is possible that circulating spirochetes are directly responsible for these effects. Indeed, we recently showed that Bt2 and its predominant outer membrane lipoprotein, Vsp2, cause apoptosis of brain microvascular endothelial cells in vitro (unpublished data). Moreover, in malaria and trypanosomiasis, it has been shown that endothelial cells can be damaged directly by these pathogens or their products (30–32). We cannot, however, rule out the possibility that factors other than the pathogen itself, including direct damage by infiltrating macrophages and/or neutrophils (Fig. 3B) or from TNF or other circulating soluble factors, may be involved. Because neutralization of TNF prevented death and partially protected the brain from injury, it is likely that reducing TNF is one important protective mechanism of IL-10 in this infection. There are several potential

explanations for the protective effect of the anti-TNF antibody in this model: systemically, neutralization of TNF restored the ability of the innate immune system to control bacteremia by preventing apoptosis of phagocytic cells, as we recently showed (24); TNF neutralization reduced the leptomeningeal inflammatory response as shown in the present study (Fig. 3H).

The importance of vascular injury as a complication of infection with pathogenic spirochetes has been recognized at least since 1922 (33), and vasculitis has been reported in humans infected with the Lyme disease spirochete *Borrelia burgdorferi* (34–36). We found vasculitis in skeletal muscle from rhesus macaques experimentally infected with *B. burgdorferi* (37) and a preferential localization of *B. burgdorferi* in the arterial wall (10). Hemorrhagic and thrombotic cerebrovascular complications are common in infection with the syphilis spirochete *Treponema pallidum* (1) and in the endemic form of relapsing fever in humans (38–42) and experimental animals (43). In relapsing fever, hemorrhage is often not limited to the brain because many patients can have epistaxis, hematuria, gastrointestinal bleeding, and skin petechiae (38,41).

An important protective role of IL-10 for the cerebral circulation has been documented in several experimental brain injury models. In cerebral malaria, IL-10 deficiency increased morbidity and mortality secondary to intracerebral hemorrhage, necrotic vasculitis, and cerebral edema (29,30,44). Interleukin 10 has also been shown to protect the brain from injury in toxoplasma encephalitis (45), African trypanosomiasis (46), *Staphylococcus aureus* brain abscess (47), pneumococcal meningitis (48), and *Listeria monocytogenes* (49). The protective role of IL-10 in the brain may occur via reduced synthesis of TNF (50). Several studies have implicated TNF in the pathogenesis of inflammatory brain injury, including human immunodeficiency virus encephalitis, cerebral malaria, and bacterial meningitis (51,52).

The present results provide experimental evidence for a fundamental protective role of IL-10 for the brain during spirochetal infection. The novel observation that the brain microcirculation is more vulnerable to spirochetal injury may be one of the reasons for the high frequency of neurological complications in these infections. Future studies should be able to determine whether IL-10 plays a similar neuro-protective role at times of lower pathogen load, as during infection with relapsing fever spirochetes in immunocompetent mice.

## Acknowledgments

This study was supported by Grant No. 1R21NS053997-01 from the National Institutes of Health and by the UMDNJ Foundation to Diego Cadavid. This research was also supported by the intramural research program of the National Institutes of Health-National Institute of Allergy and Infectious Diseases. The content of this publication does not necessarily reflect the views or policies of the Department of Health and Human Services, nor does mention of trade names, commercial products, or organizations imply endorsement by the US Government.

## REFERENCES

1. Cadavid, D.; Pachner, AR. Neurosyphilis. In: Griggs, RC.; Joynt, RJ., editors. Clinical Neurology. Philadelphia, PA: Lippincott-Raven; 2000. p. 1-43.
2. Anderson T, Zimmerman L. Relapsing fever in Korea. A clinicopatho-logic study of eleven fatal cases with special attention to association with Salmonella infections. Am J Pathol 1955;31:1083–1109. [PubMed: 13268613]
3. Southern P, Sanford J. Relapsing fever. Medicine 1969;48:129–149.
4. Cadavid D, Barbour AG. Neuroborreliosis during relapsing fever: Review of the clinical manifestations, pathology, and treatment of infections in humans and experimental animals. Clin Infect Dis 1998;26:151–164. [PubMed: 9455525]
5. Cadavid, D. Lyme disease and relapsing fever. In: Scheld, W.; Whitley, R.; Marra, C., editors. Infections of the Central Nervous System. Philadelphia, PA: Lippincott-Raven; 2004. p. 659-690.

6. Marra CM, Castro CD, Kuller L, et al. Mechanisms of clearance of *Treponema pallidum* from the CSF in a nonhuman primate model. Neurology 1998;51:957–961. [PubMed: 9781512]
7. England JD, Bohm RP Jr, Roberts ED, Philipp MT. Lyme neuro-borreliosis in the rhesus monkey. Semin Neurol 1997;17:53–56. [PubMed: 9166960]
8. Roberts ED, Bohm RP Jr, Cogswell FB, et al. Chronic Lyme disease in the rhesus monkey. Lab Invest 1995;72:146–160. [PubMed: 7853849]
9. Bai Y, Narayan K, Dail D, et al. Spinal cord involvement in the nonhuman primate model of Lyme disease. Lab Invest 2004;84:160–172. [PubMed: 14688796]
10. Cadavid D, O'Neill T, Schaefer H, et al. Localization of *Borrelia burgdorferi* in the nervous system and other organs in a nonhuman primate model of Lyme disease. Lab Invest 2000;80:1043–1054. [PubMed: 10908149]
11. Pachner AR, Cadavid D, Shu G, et al. Central and peripheral nervous system infection, immunity, and inflammation in the NHP model of Lyme borreliosis. Ann Neurol 2001;50:330–338. [PubMed: 11558789]
12. Pachner AR, Dail D, Bai Y, et al. Genotype determines phenotype in experimental Lyme borreliosis. Ann Neurol 2004;56:361–370. [PubMed: 15349863]
13. Gelderblom H, Schmidt J, Londono D, et al. Role of interleukin 10 during persistent infection with the relapsing fever spirochete *Borrelia turicatae*. Am J Pathol 2007;170:251–262. [PubMed: 17200198]
14. Cadavid D, Garcia E, Gelderblom H. Coinfection with *Borrelia turicatae* serotype 2 prevents the severe vestibular dysfunction and earlier mortality caused by serotype 1. J Infect Dis 2007;195:1686–1693. [PubMed: 17471439]
15. Cadavid D, Pachner AR, Estanislao L, et al. Isogenic serotypes of *Borrelia turicatae* show different localization in the brain and skin of mice. Infect Immun 2001;69:3389–3397. [PubMed: 11292762]
16. Cadavid D, Thomas DD, Crawley R, et al. Variability of a bacterial surface protein and disease expression in a possible mouse model of systemic Lyme borreliosis. J Exp Med 1994;179:631–642. [PubMed: 8294872]
17. Sethi N, Sondey M, Bai Y, et al. Interaction of a neurotropic strain of *Borrelia turicatae* with the cerebral microcirculation system. Infect Immun 2006;74:6408–6418. [PubMed: 16940140]
18. Cadavid D, Bundoc V, Barbour AG. Experimental infection of the mouse brain by a relapsing fever *Borrelia* species: A molecular analysis. J Infect Dis 1993;168:143–151. [PubMed: 8515101]
19. Cadavid D, Sondey M, Garcia E, et al. Residual brain infection in relapsing fever borreliosis. J Infect Dis 2006;193:1451–1458. [PubMed: 16619194]
20. Larsson C, Andersson M, Pelkonen J, et al. Persistent brain infection and disease reactivation in relapsing fever borreliosis. Microbes Infect 2006;8:2213–2219. [PubMed: 16782384]
21. Gelderblom H, Londono D, Bai Y, et al. High production of CXCL13 in blood and brain during persistent infection with the relapsing fever spirochete *Borrelia turicatae*. J Neuropathol Exp Neurol 2007;66:208–217. [PubMed: 17356382]
22. Cooper PJ, Fekade D, Remick DG, et al. Recombinant human interleukin-10 fails to alter proinflammatory cytokine production or physiologic changes associated with the Jarisch-Herxheimer reaction. J Infect Dis 2000;181:203–209. [PubMed: 10608768]
23. Londoño D, Bai Y, Zuckert WR, et al. Cardiac apoptosis in severe relapsing fever borreliosis. Infect Immun 2005;73:7669–7676. [PubMed: 16239571]
24. Londoño D, Marques A, Hornung R, et al. IL-10 helps control pathogen load during high-level bacteremia. J Immunol. 2008In press
25. Cadavid D, Pennington PM, Kerentseva TA, et al. Immunologic and genetic analyses of VmpA of a neurotropic strain of *Borrelia turicatae*. Infect Immun 1997;65:3352–3360. [PubMed: 9234797]
26. Pennington PM, Cadavid D, Barbour AG. Characterization of VspB of *Borrelia turicatae*, a major outer membrane protein expressed in blood and tissues of mice. Infect Immun 1999;67:4637–4645. [PubMed: 10456910]
27. Hesse M, Piccirillo CA, Belkaid Y, et al. The pathogenesis of schistosomiasis is controlled by cooperating IL-10-producing innate effector and regulatory T cells. J Immunol 2004;172:3157–3166. [PubMed: 14978122]

28. Kullberg MC, Rothfuchs AG, Jankovic D, et al. *Helicobacter hepaticu-s*-induced colitis in interleukin-10-deficient mice: Cytokine requirements for the induction and maintenance of intestinal inflammation. Infect Immun 2001;69:4232–4241. [PubMed: 11401959]
29. Li C, Sanni LA, Omer F, et al. Pathology of *Plasmodium chabaudi chabaudi* infection and mortality in interleukin-10-deficient mice are ameliorated by anti-tumor necrosis factor alpha and exacerbated by anti-transforming growth factor beta antibodies. Infect Immun 2003;71:4850–4856. [PubMed: 12933825]
30. Hunt NH, Golenser J, Chan-Ling T, et al. Immunopathogenesis of cerebral malaria. Int J Parasitol 2006;36:569–582. [PubMed: 16678181]
31. Potter S, Chan-Ling T, Ball HJ, et al. Perforin mediated apoptosis of cerebral microvascular endothelial cells during experimental cerebral malaria. Int J Parasitol 2006;36:485–496. [PubMed: 16500656]
32. Stiles JK, Whittaker J, Sarfo BY, et al. Trypanosome apoptotic factor mediates apoptosis in human brain vascular endothelial cells. Mol Biochem Parasitol 2004;133:229–240. [PubMed: 14698435]
33. Wail S. Virchows. Arch Path Anat Physiol 1922;240:261.
34. Camponovo F, Meier C. Neuropathy of vasculitic origin in a case of Garin-Boujadoux-Bannwarth syndrome with positive borrelia antibody response. J Neurol 1986;233:69–72. [PubMed: 3009723]
35. Keil R, Baron R, Kaiser R, et al. Vasculitis course of neuroborreliosis with thalamic infarct [in German]. Nervenarzt 1997;68:339–341. [PubMed: 9273464]
36. Oksi J, Kalimo H, Marttila RJ, et al. Inflammatory brain changes in Lyme borreliosis. A report on three patients and review of literature. Brain 1996;119:2143–2154. [PubMed: 9010017]
37. Cadavid D, Bai Y, Dail D, et al. Infection and inflammation in skeletal muscle from nonhuman primates infected with different genospecies of the Lyme disease spirochete *Borrelia burgdorferi*. Infect Immun 2003;71:7087–7098. [PubMed: 14638799]
38. Ahmed MA, Abdel Wahab SM, Abdel Malik MO, et al. Louse-borne re-lapsing fever in the Sudan. A historical review and a clinico-pathological study. Trop Geogr Med 1980;32:106–111. [PubMed: 7423600]
39. Bryceson AD, Parry EH, Perine PL, et al. Louse-borne relapsing fever. Q J Med 1970;39:129–170. [PubMed: 4913454]
40. Judge DM, Samuel I, Perine PL, et al. Louse-borne relapsing fever in man. Arch Pathol 1974;97:136–170. [PubMed: 4811584]
41. Perine PL, Parry EH, Vukotich D, et al. Bleeding in louse-borne relapsing fever. I. Clinical studies in 37 patients. Trans R Soc Trop Med Hyg 1971;65:776–781. [PubMed: 5157439]
42. Salih SY, Mustafa D, Abdel Wahab SM, et al. Louse-borne relapsing fever: I. A clinical and laboratory study of 363 cases in the Sudan. Trans R Soc Trop Med Hyg 1977;71:43–48. [PubMed: 871032]
43. Babes V. Hemorragies meningees et autres manifestations hemorragiques dans la fievre recurrente. C R Soc Biol 1916;79:855–857.
44. Sanni LA, Jarra W, Li C, et al. Cerebral edema and cerebral hemorrhages in interleukin-10-deficient mice infected with *Plasmodium chabaudi*. Infect Immun 2004;72:3054–3058. [PubMed: 15102820]
45. Wilson EH, Wille-Reece U, Dzierszinski F, et al. A critical role for IL-10 in limiting inflammation during toxoplasmic encephalitis. J Neuroimmunol 2005;165:63–74. [PubMed: 16005735]
46. Sternberg JM, Rodgers J, Bradley B, et al. Meningoencephalitic African trypanosomiasis: Brain IL-10 and IL-6 are associated with protection from neuro-inflammatory pathology. J Neuroimmunol 2005;167:81–89. [PubMed: 16054238]
47. Stenzel W, Dahm J, Sanchez-Ruiz M, et al. Regulation of the inflammatory response to *Staphylococcus aureus*-induced brain abscess by interleukin-10. J Neuropathol Exp Neurol 2005;64:1046–1057. [PubMed: 16319715]
48. van Furth AM, Seijmonsbergen EM, Langermans JA, et al. High levels of interleukin 10 and tumor necrosis factor alpha in cerebrospinal fluid during the onset of bacterial meningitis. Clin Infect Dis 1995;21:220–222. [PubMed: 7578738]
49. Deckert M, Soltek S, Geginat G, et al. Endogenous interleukin-10 is required for prevention of a hyperinflammatory intracerebral immune response in *Listeria monocytogenes* meningoencephalitis. Infect Immun 2001;69:4561–4571. [PubMed: 11402000]

50. Buch T, Uthoff-Hachenberg C, Waisman A. Protection from autoimmune brain inflammation in mice lacking IFN-regulatory factor-1 is associated with Th2-type cytokines. Int Immunol 2003;15:855–859. [PubMed: 12807824]

51. Dziedzic T, Bartus S, Klimkowicz A, et al. Intracerebral hemorrhage triggers interleukin-6 and interleukin-10 release in blood. Stroke 2002;33:2334–2335. [PubMed: 12215608]

52. Dziegielewska KM, Moller JE, Potter AM, et al. Acute-phase cytokines IL-1beta and TNF-alpha in brain development. Cell Tissue Res 2000;299:335–345. [PubMed: 10772248]

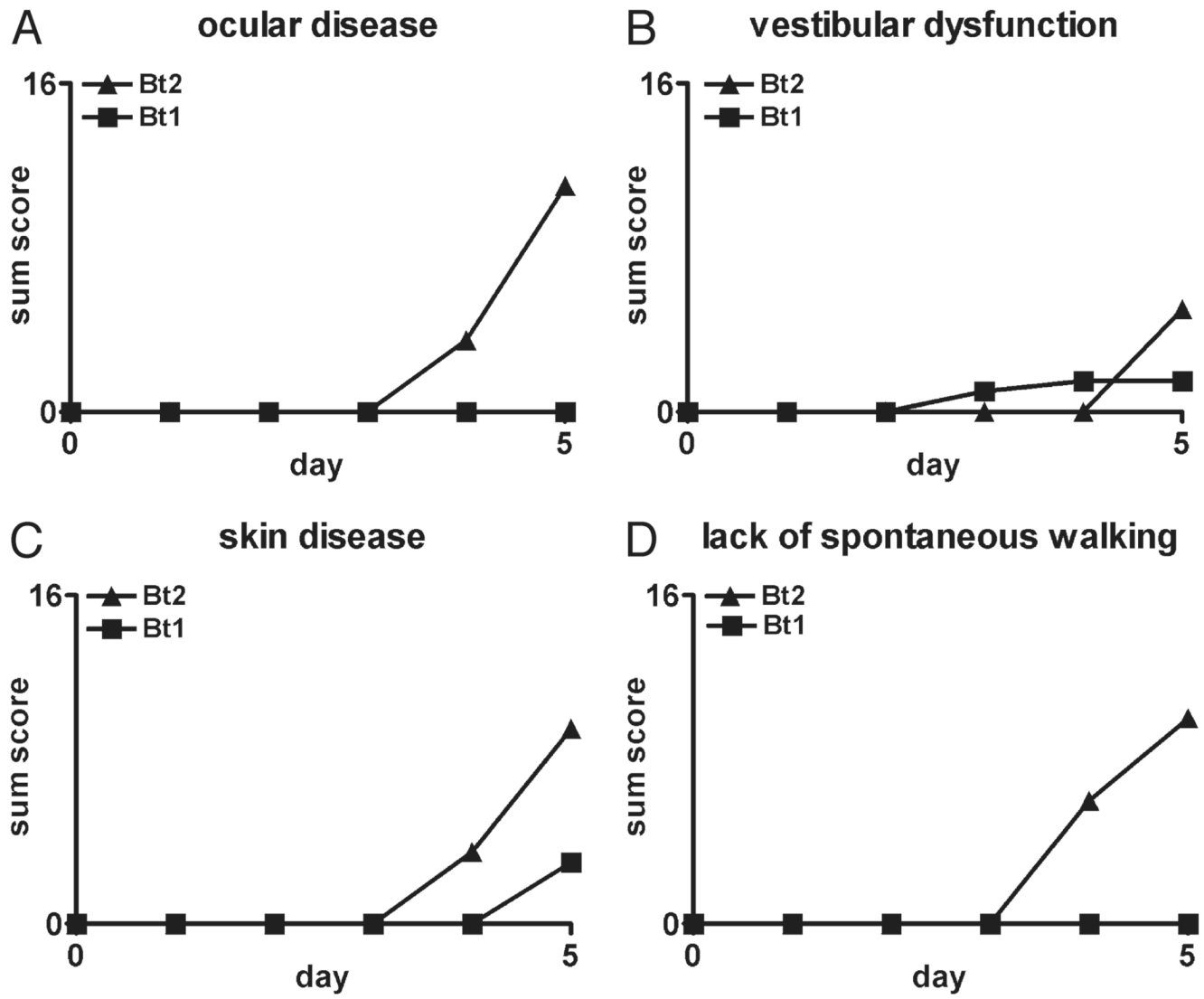


**FIGURE 1.**

Disease in RAG2/IL-10$^{-/-}$ mice infected with *Borrelia turicatae* isogenic serotype 1 (Bt1) or 2 (Bt2). Disease severity in the eyes **(A)**, vestibular system **(B)**, and skin **(C)**, and activity level **(D)** were assessed daily over 5 days as described in the Materials and Methods section in RAG2/IL-10$^{-/-}$ mice infected with Bt1 or Bt2 of *Borrelia turicatae*. For each graph, the highest value on the y axis equals the maximum possible sum score per group (n = 8 mice per group).

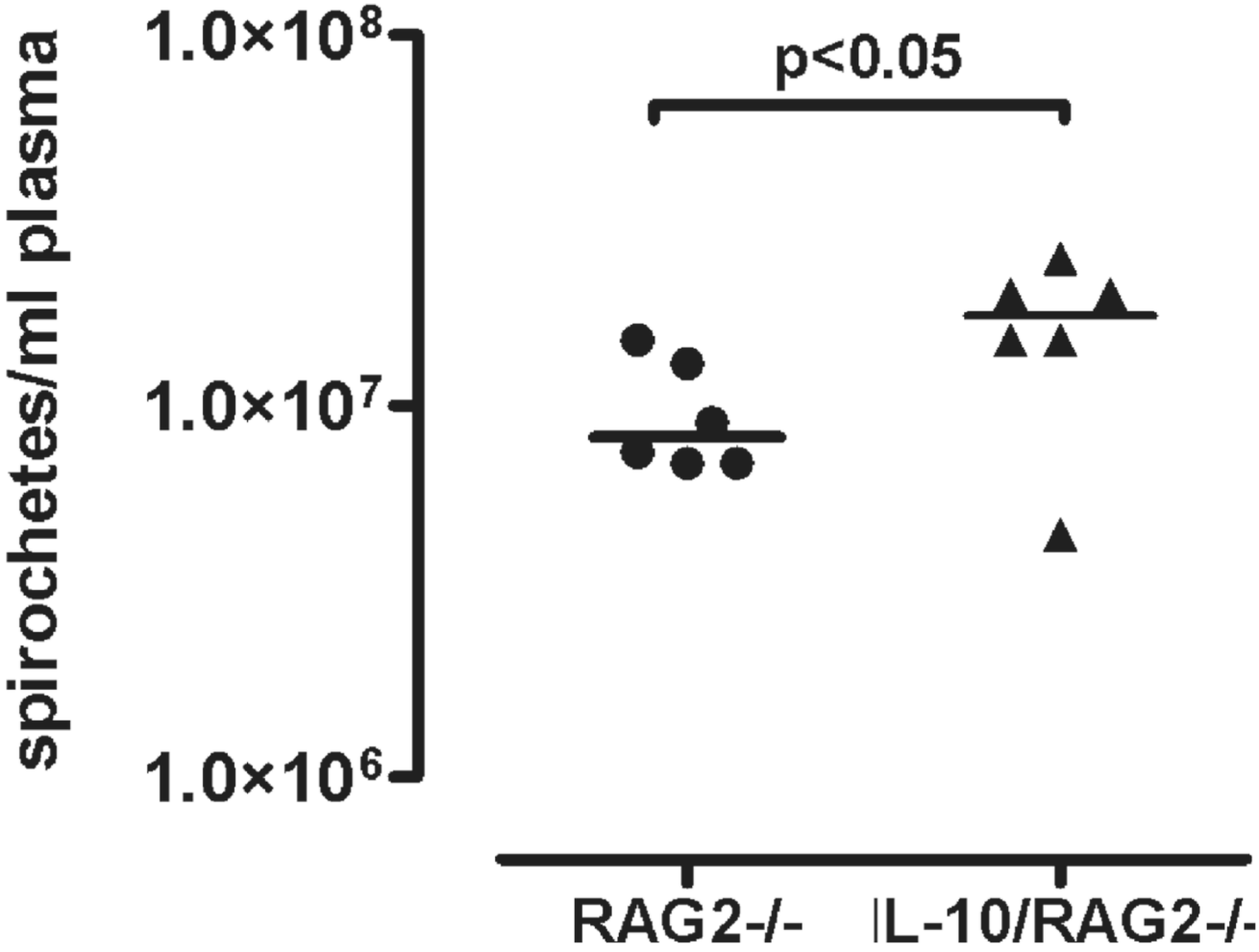


**FIGURE 2.**

Pathogen load in the blood of RAG2$^{-/-}$ and RAG2/IL-10$^{-/-}$ mice infected with *Borrelia turicatae* isogenic serotype 1. The pathogen load in the blood was determined by counting spirochetes with a Petroff-Hausser chamber in necropsy plasma 12 days after inoculation of *Borrelia turicatae* isogenic serotype 1 in RAG2$^{-/-}$ (n = 6) or RAG2/IL-10$^{-/-}$ (n = 6) mice. The horizontal bar indicates the mean, and each dot or triangle represents an individual mouse.

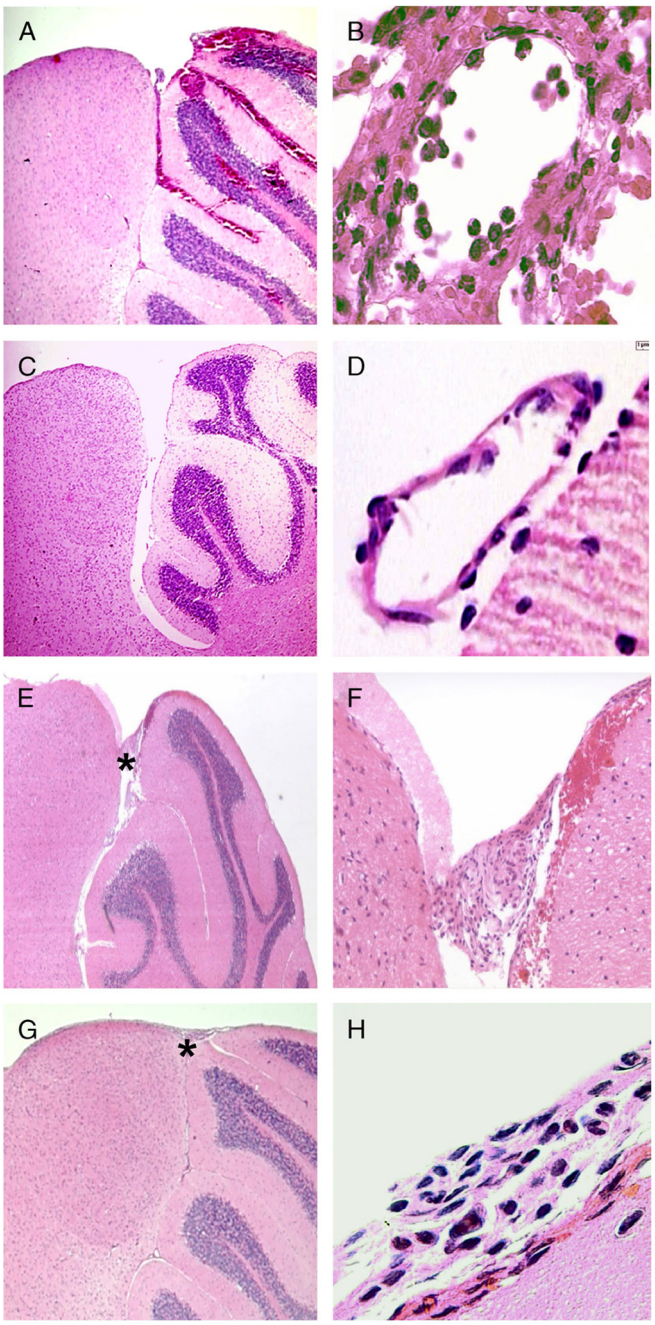


**FIGURE 3.**

Pathological findings in the brains of RAG2/IL-10$^{-/-}$ mice infected with *Borrelia turicatae* isogenic serotype 1 (Bt1) or 2 (Bt2). *(A, B)* Hematoxylin and eosin (H&E)-stained sections of the brain of a Bt2-infected RAG2/IL-10$^{-/-}$ mouse examined on Day 5 after inoculation. Extensive subarachnoid and intraparenchymal hemorrhages at low magnification (original magnification: **[A]** 200×). Leptomeningeal micro-vessel with prominent infiltration by inflammatory cells in a region of subarachnoid hemorrhage (original magnification: **[B]** 1,000×). **(C, D)** H&E-stained sections of the brain of a Bt2-infected RAG2$^{-/-}$ mouse on Day 5 after inoculation show no evidence of hemorrhage or vasculitis. **(E, F)** H&E-stained midsagittal sections of the brain from a Bt1-infected RAG2/IL-10$^{-/-}$ mice examined 12 days

after inoculation. Low-magnification view shows an area of leptomeningeal hemorrhage near the superior cerebellum without parenchymal hemorrhage (original magnification: **[E]** 200×). Higher magnification of the area shown by the asterisk in **(E)** shows subarachnoid hemorrhage and blood vessel thrombosis (original magnification: **[F]** 400×). **(G, H)** H&E-stained sections of the brain of a Bt2-infected IL-10/RAG2$^{-/-}$ mouse treated with anti-tumor necrosis factor antibody and necropsied on Day 12 after inoculation with Bt2. Note the absence of subarachnoid or intraparenchymal hemorrhage (original magnification: **[G]** 200×). Higher magnification of the area shows infiltration by inflammatory cells and subtle subarachnoid hemorrhage (original magnification: **[H]** 1,000×).

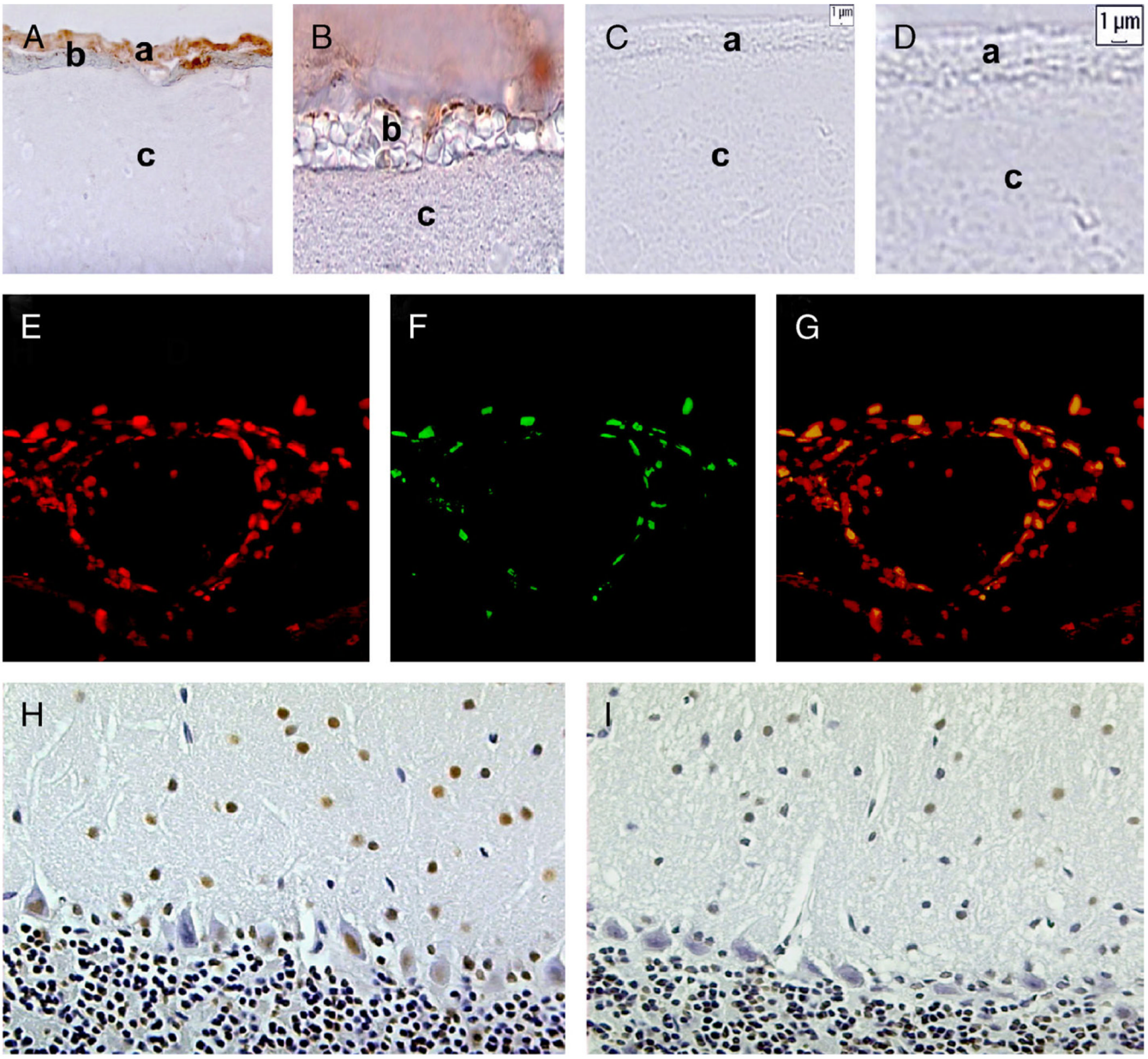


**FIGURE 4.**

Terminal transferase-mediated DNA nick end-labeling (TUNEL) staining in the brains of RAG2$^{-/-}$ and RAG2/IL-10$^{-/-}$ mice infected with isogenic serotype 1 (Bt1) or 2 (Bt2). The TUNEL staining of midsagittal brain sections from a RAG2/IL-10$^{-/-}$ **(A, B)** and RAG2$^{-/-}$ **(C, D)** mice infected with Bt2 and examined on Day 5 after inoculation. The location of the leptomeninges, subarachnoid hemorrhage, and brain parenchyma are shown by letters a, b, and c, respectively. There is prominent TUNEL staining of leptomeningeal cells only in the Bt2-infected RAG2/IL-10$^{-/-}$ mouse **(A, B,** diaminobenzidine (DAB) chromogen). Note that apoptotic endothelial cells are prominent in the area of subarachnoid hemorrhage. Cryostat sections of the brain of a Bt2-infected RAG2/IL-10$^{-/-}$ mouse were also stained by immunofluorescence with TUNEL (red panel **[E]**) and isolectin B4 (green panel **[F]**). **(G)** Panel shows the merged images of **(E)** and **(F)** (yellow indicates colocalization). The TUNEL staining

(DAB chromogen) in the cerebellum of Bt1-infected RAG2/IL-$10^{-/-}$ **(H)** and $RAG2^{-/-}$ **(I)** mice examined on Day 12 after inoculation.

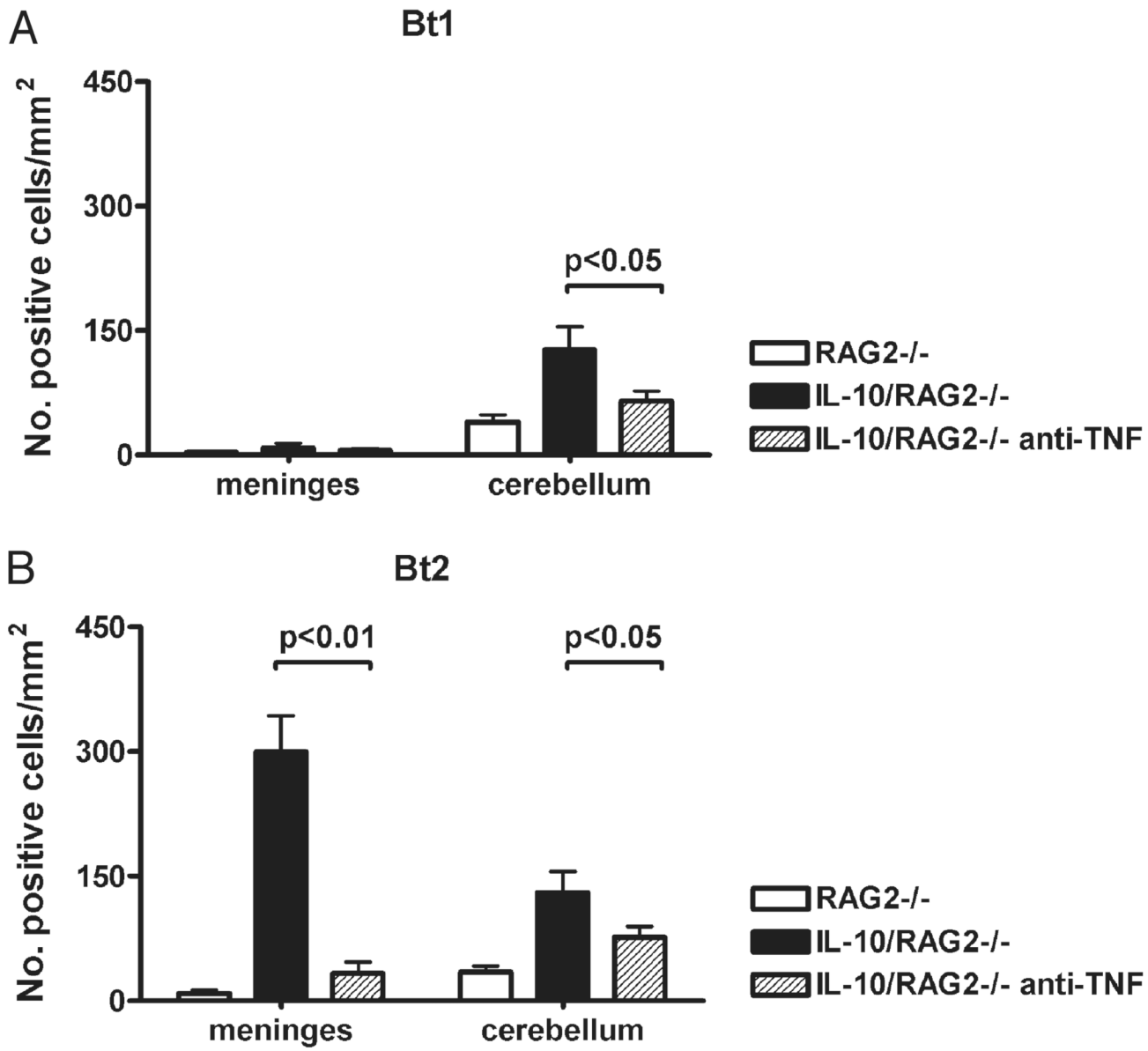


**FIGURE 5.**

Terminal transferase-mediated DNA nick end-labeling (TUNEL) staining in the brain of RAG2/IL-10$^{-/-}$ mice infected with *Borrelia turicatae*. The numbers of stained cells in the leptomeninges and cerebellar molecular layer were counted in TUNEL-stained midsagittal brain sections from RAG2$^{-/-}$ (n = 3) and RAG2/IL-10$^{-/-}$ (n = 3) mice infected with serotype 1 (Bt1 **[A]**) or 2 (Bt2 **[B]**) of *Borrelia turicatae*. One group of mice in each group had been treated with anti-TNF-neutralizing antibody. Results are expressed as mean (SD) stained cells per square millimeter.

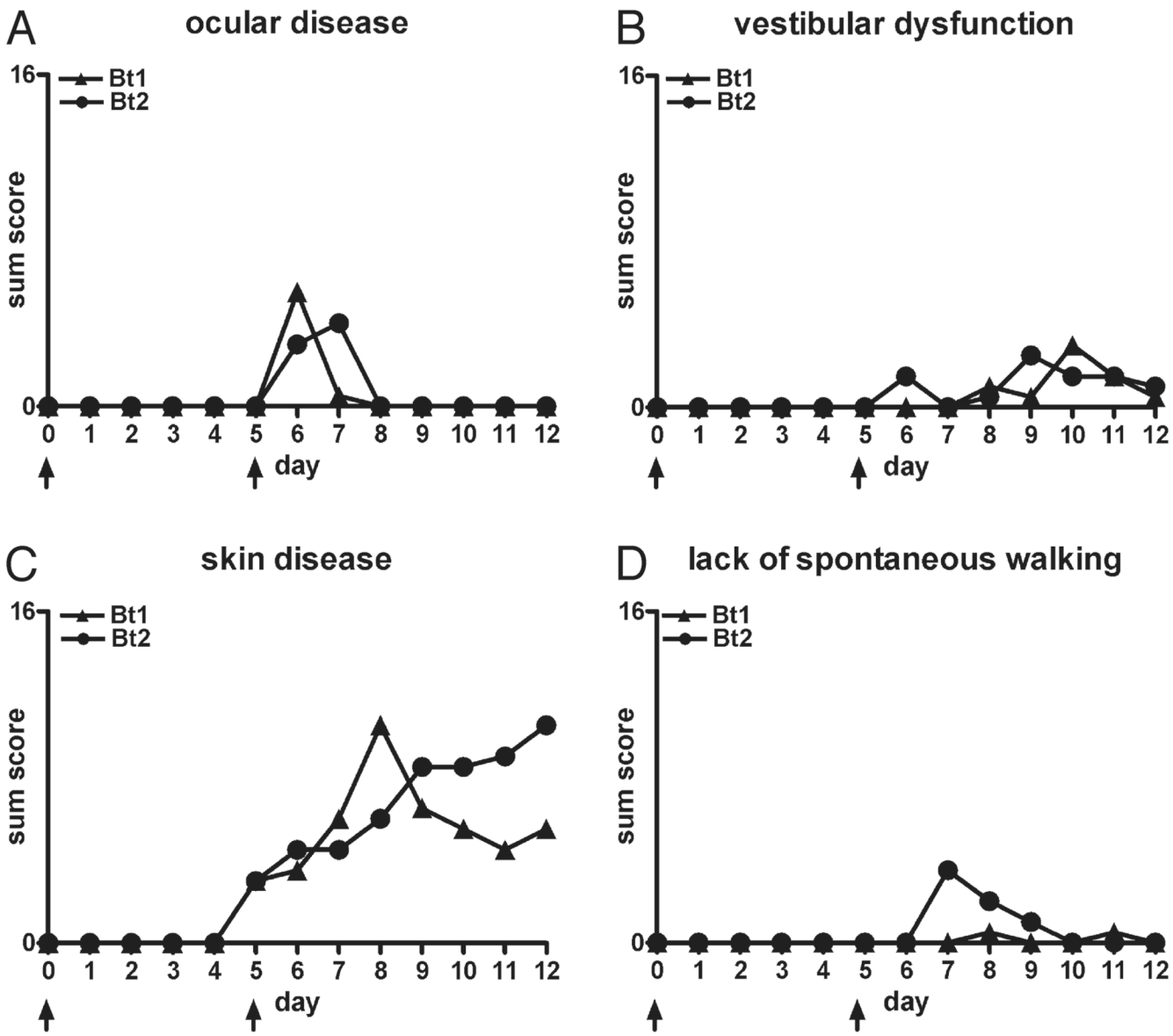


**FIGURE 6.**

Effect of neutralization of TNF on clinical disease in RAG2/IL-10$^{-/-}$ mice infected with isogenic serotype 1 (Bt1) or 2 (Bt2). Six RAG2/IL-10$^{-/-}$ mice were inoculated with Bt1 or Bt2 of *Borrelia turicatae* and examined daily for signs of clinical disease in the skin, eyes, and vestibular system, and for spontaneous locomotor activity for 12 days. The examiner was blinded to infection and genotype. Results are expressed as sum score per group. The y axis shows the maximum possible sum score. The arrows show the day of administration of anti-TNF-neutralizing antibody.

**TABLE**

Pathological Findings in the Brains of Bt1-Infected and Bt2-Infected Mice

| Genotype | Anti-TNF* | Inoculum | Hemorrhage | Vasculitis | Thrombosis | Meningitis |
|---|---|---|---|---|---|---|
| RAG2$^{-/-}$ | No | PBS | 0/4 | 0/4 | 0/4 | 0/4 |
| | No | Bt2 | 0/8 | 0/8 | 0/8 | 0/8 |
| | No | Bt1 | 0/6 | 0/6 | 0/6 | 0/6 |
| RAG2/IL-10$^{-/-}$ | No | PBS | 0/4 | 0/4 | 0/4 | 0/4 |
| | No | Bt1 | 2/6 | 0/6 | 3/6 | 1/6 |
| | Yes | Bt1 | 1/6 | 1/6 | 0/6 | 1/6 |
| | No | Bt2† | 5/8 | 6/8 | 0/8 | 4/8 |
| | Yes | Bt2 | 2/6 | 3/6 | 3/6 | 6/6 |

*Some mice were treated with 0.75 mg of anti-TNF-neutralizing antibody on Days 0 and 5 after inoculation of Bt1 or Bt2.

RAG2$^{-/-}$ and RAG2/IL-10$^{-/-}$ mice inoculated with Bt2 and without anti-TNF treatment died or were killed on Day 5; all other mice were killed on Day 12 after inoculation.